Polymer Chemistry

PAPER

View Article Online
View Journal | View Issue

Cite this: *Polym. Chem.*, 2026, **17**, 1807

Carboxylic acid α-end-functionalized poly(2-oxazoline)s synthesized through benzylic CROP initiators

Caroline T. Holick, [a,b] Nora Engel, [a,b] Nicole Fritz,[a,b] Christine Weber [a,b] and Ulrich S. Schubert *[a,b,c,d]

The increasing significance of poly(2-oxazoline)s (POx) as a replacement for poly(ethylene glycol) in biomedical applications has triggered a need for end-functionalized building blocks that can be functionalized with components such as targeting ligands, labels, or other polymers. In the present study, we introduce methyl esters at the α-chain end of hydrophilic poly(2-ethyl-2-oxazoline) (PEtOx) as well as hydrophobic poly(2-*n*-nonyl-2-oxazoline) (PNonOx) through the utilization of two bromomethylbenzoates as initiators for the cationic ring-opening polymerization (CROP) of the corresponding monomers. Kinetic studies revealed that the *meta*-substituted compound was superior to the *para*-substituted compound as it enabled faster initiation of the CROP. Detailed studies of the end-group fidelity by NMR spectroscopy, matrix-assisted laser desorption ionization mass spectrometry and high-performance liquid chromatography revealed that PEtOx obtained through CROP at 140 °C contained >20% proton-initiated chains lacking the end group of interest due to the occurrence of chain transfer reactions. The chain transfer was almost absent when the CROP was performed at 85 °C in acetonitrile. Methyl-3-(bromomethyl)benzoate was further applied to obtain block copolymers comprising PEtOx and PNonOx, as well as heterotelechelic PEtOx through termination of the CROP with triethylammonium acetate and sodium azide, respectively. Hydrolysis using aqueous NaOH yielded PEtOx with carboxylic acid α- and azide or hydroxyl ω-end groups. As high end-group fidelities were achieved, the simple commercial initiator opens a new and straightforward route towards various building blocks for advanced POx architectures, in particular with respect to the orthogonal reactivity of carboxylic acid or methyl ester and azide end groups.

Received 30th March 2026,
Accepted 1st April 2026

DOI: 10.1039/d6py00309e

rsc.li/polymers

Introduction

For many years, poly(ethylene glycol) (PEG) has been the gold standard for biomedical applications.[1] However, recent studies proving the formation of anti-PEG antibodies, which can cause hypersensitivity reactions, have led to the search for a suitable alternative.[2] Poly(2-oxazoline)s (POx) have gathered significant attention in that respect. In particular, POx with methyl and ethyl side chains exhibit properties similar to those of PEG, including biocompatibility, hydrophilicity, and most importantly, the stealth effect.[3–5] Their capacity for facile adaptability through modification of the side chains or the end groups makes POx of considerable interest, in particular in the field of drug delivery.[4,6] The versatility of POx is rooted in cationic ring-opening polymerization (CROP), which enables control over the chain length as well as the end groups.[6,7] The introduction of various types of end groups into the POx chain can be accomplished by the utilization of suitable termination agents and initiators.[8] Examples include amino or hydroxyl groups,[9–12] azides,[13,14] thiols,[12,15] alkynes[16,17] and cyclooctynes[18] useful to attach other functional moieties or building blocks to the POx.

Carboxylic acids are of critical importance in the bioconjugation field, serving as versatile functional groups for the covalent attachment of drugs, fluorescent probes and biomolecules such as proteins through well-established amidation reactions.[19] The introduction of carboxylic acids into substituents along the POx backbone has been exploited by CROP of monomers featuring methyl esters, such as methyl 3-(4,5-dihydrooxazol-2-yl)propanoate (MestOx), and successive hydrolysis of the methyl ester moiety.[20,21] The attachment of a carboxylate at the ω-chain end of POx can be achieved either through termination of the CROP with nucleophiles that

[a]*Laboratory of Organic and Macromolecular Chemistry (IOMC), Friedrich Schiller University Jena, Humboldtstrasse 10, 07743 Jena, Germany. E-mail: ulrich.schubert@uni-jena.de*
[b]*Jena Center for Soft Matter (JCSM), Friedrich Schiller University Jena, Philosophenweg 7, 07743 Jena, Germany*
[c]*Helmholtz Institute for Polymers in Energy Applications Jena (HIPOLE Jena), Lessingstraße 12–14, 07743 Jena, Germany*
[d]*Helmholtz-Zentrum Berlin für Materialien und Energie GmbH (HZB), Hahn-Meitner-Platz 1, 14109 Berlin, Germany*

include methyl ester moieties, or *via* a series of post-polymerization functionalization reactions using, *e.g.*, succinic anhydride.[22–24]

Surprisingly, there are only a few reports describing access to POx with α-COOH groups through the use of functionalized CROP initiators (Fig. 1). Examples include methyl bromoacetate,[25] *tert*-butyl bromoacetate[26] and ethyl 3-bromopropionate.[23] All these initiators represent alkyl esters as an unprotected carboxylic acid can act as a nucleophile and terminate the CROP. Hence, the compounds introduce a protected carboxylic acid moiety, which can be deprotected subsequently, offering a viable strategy for α-end group functionalization. However, they tend to exhibit slow initiation of the CROP, as it has been demonstrated in a detailed kinetic study conducted for methyl bromoacetate.[25] In contrast, benzyl bromides are capable of fast CROP initiation,[27] as the resonance stabilization of benzyl cations promotes nucleophilic substitutions at benzyl substrates. In fact, benzyl bromides with additional methyl ester substituents on the benzene ring are commercially available but have, to the best of our knowledge, not yet been investigated as initiators for the CROP of 2-oxazolines. For these molecules, the position of the methyl ester on the aromatic ring might influence the initiation capability as the methyl ester is not decoupled electronically (Scheme S1).

In this study, we explored if methyl-4-(bromomethyl)benzoate (**4M**) and methyl-3-(bromomethyl)benzoate (**3M**) are feasible CROP initiators and able to produce well-defined POx with carboxylic acid α-end groups. To thoroughly evaluate their performance, detailed kinetic studies were carried out to assess the initiation efficiency and propagation rate constants using hydrophilic as well as hydrophobic monomers. The end-group fidelity of the resulting POx was determined by means of high-performance liquid chromatography (HPLC) hyphenated to matrix-assisted laser desorption ionization time-of-flight mass spectrometry (MALDI-TOF MS). Ultimately, we present the synthesis of amphiphilic block copolymers and heterotelechelic building blocks based on optimized CROP conditions using the novel initiators (Scheme 1).

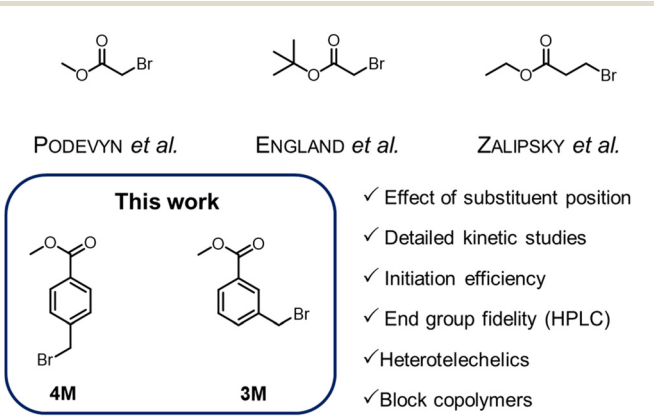

Fig. 1 Schematic representation of initiators used in previous works and in this study.

Experimental

Materials

2-Ethyl-2-oxazoline (EtOx, Sigma-Aldrich, ≥99%) was distilled under an argon atmosphere. 2-*n*-Nonyl-2-oxazoline (NonOx, >99%, water content <70 ppm) was a gift from NGP Polymers and was used as received. Methyl-4-(bromomethyl)benzoate (**4M**, >97%) and methyl-3-(bromomethyl)benzoate (**3M**, >97%) were purchased from TCI and recrystallized in *n*-hexane. Acetic acid (AcOH, VWR, ACS, Reag. Ph. Eur.), triethylamine (NEt_3, Sigma-Aldrich, ≥99%), sodium hydroxide (NaOH, Roth, ≥99%) and sodium azide (abcr, 99%) were used as received.

Acetonitrile (CH_3CN) used as the CROP solvent was either dried using a solvent purification system (SPS 800, MBRAUN) or purchased from Roth (Rotidry®Sept ≥99.9%, ≤10 ppm H_2O). All other chemicals were obtained from standard suppliers and used without further purification.

Instrumentation

Proton nuclear magnetic resonance (^{1}H NMR) spectra were recorded using a Bruker AC 300 MHz spectrometer at room temperature in $CDCl_3$. The residual non-deuterated solvent signal was used for referencing the chemical shift (δ).

Size-exclusion chromatography (SEC) measurements were conducted on a Shimadzu system equipped with a CBM-20A system controller, an LC-10AD VP pump, a SIL-10AD VP autosampler, a RID-10A refractive index detector, a TCC6000 column oven from Techlab, and an SDV Linear S column from PSS at 40 °C using $CHCl_3$: NEt_3 : isopropanol (94 : 4 : 2) as the eluent at a flow rate of 1 mL min^{-1}. Polystyrene (PS) standards from Polymer Standards Service (400 to 1 000 000 g mol^{-1}) were used for calibration.

Matrix-assisted laser desorption ionization time-of-flight mass spectrometry (MALDI-TOF MS) was carried out on a rapifleX MALDI-TOF/TOF system from Bruker Daltonics equipped with a smartbeam™ 3D laser (355 nm wavelength). The spectra were recorded in the positive reflector mode. *trans*-2-[3-(4-*tert*-Butylphenyl)-2-methyl-2-propenylidene]malononitrile (DCTB) was used as the matrix, and sodium trifluoroacetate was added as a doping salt. Evaluation and processing of the recorded spectra were performed using the manufacturer's software flexAnalysis 4.0 including baseline subtraction and calibration using the poly(methyl methacrylate) (PMMA) standard from Polymer Standards Service (2500 g mol^{-1} or 5000 g mol^{-1}).

Gas chromatography (GC) measurements were performed on a Shimadzu GC-2010 Plus system equipped with an AOC-20s autosampler, an AOC-20i injector and a flame ionization detector (FID) using chloroform as the solvent and helium as the carrier gas. The separation was carried out on a Phenomenex ZB-5 column as the stationary phase (5% phenyl, 95% dimethyl polysiloxane, 30 m length, 0.25 mm inner diameter and 0.25 μm film thickness). GC was performed using the following parameters: FID temperature 270 °C, split 10%, injection volume 0.2 μL; program: 2 min at 60 °C, heating at 16 °C min^{-1} up to 200 °C, hold for 4 min at 200 °C. Monomer

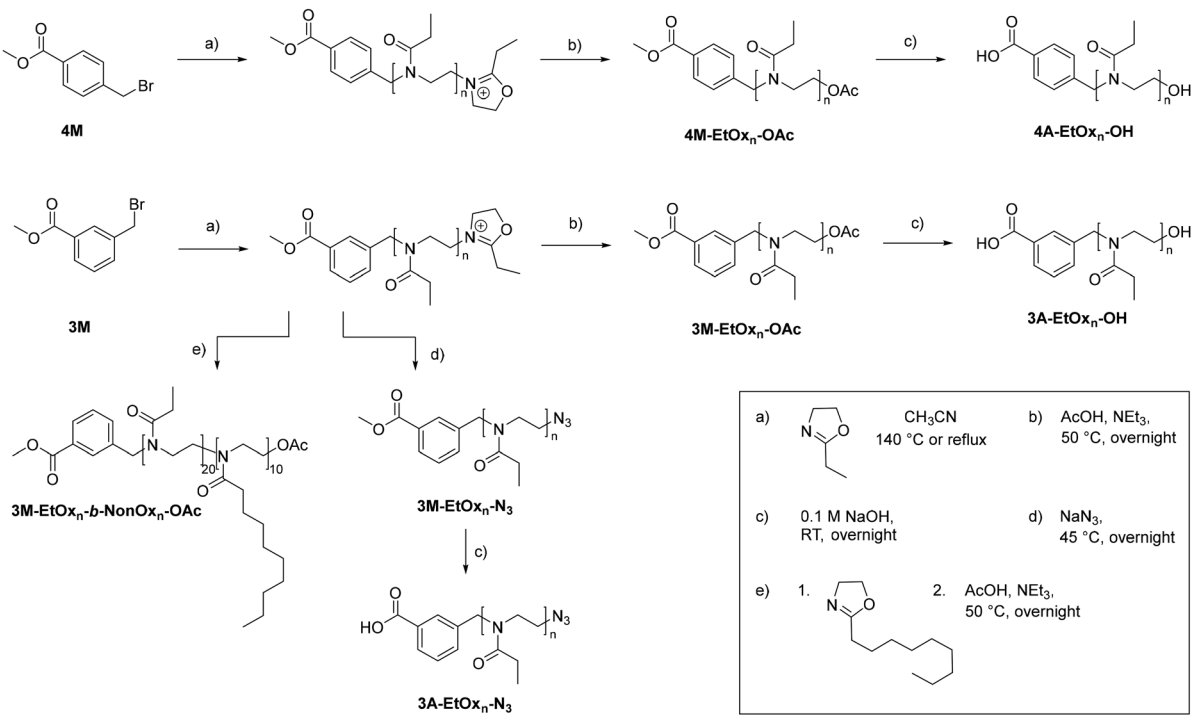

Scheme 1 Schematic representation of the CROP of 2-oxazolines initiated by **4M** and **3M** (a) including chain extensions (e), termination reactions (b, d) and post-polymerization deprotection (c) used to obtain POx with α-terminal carboxylic acid moieties.

conversions and $[M]_0/[M]_t$ were determined from the peak areas of the monomer and the CROP solvent, using the reaction solvent as an internal standard.

High-performance liquid chromatography (HPLC) was performed using an Agilent LC system 1200 series (Polymer Standards Service GmbH, Mainz, Germany), equipped with a column oven from Techlab K7 and an evaporative light scattering detector (ELSD) from SofTA Corporation, Model 400. A Chromolith High Resolution RP18 column (100 × 4.6 mm) from Merck (Darmstadt, Germany) was used as the separation column. The mobile phase consisted of A: water + 0.1% formic acid and B: acetonitrile + 0.1% formic acid. Unless stated otherwise, all samples were prepared at concentrations of 1.0 mg mL^{-1} in the mobile phase composition at the beginning of the linear gradient elution program. The injection volume was 10 μL. The flow rate was set to 1 mL min^{-1} and the column was tempered to 30 °C. After an equilibration time of 15 min with 10% B, gradient elution was done within 20 min to 90% B, followed by an isocratic step of 10 min with 90% B and a backflush within 5 min to 10% B. The ELSD was operated with nitrogen as the carrier gas (spray chamber 45 °C, drift tube temperature 70 °C).

Kinetic studies of the CROP of EtOx initiated by 4M and 3M at 140 °C

According to an $[EtOx]_0:[initiator]_0$ ratio of 20 and a concentration of EtOx of 2 mol L^{-1}, stock solutions containing EtOx (3 g, 30 mmol, 20 eq.), **4M** or **3M** (345 mg, 1.5 mmol, 1 eq.) and CH_3CN (12 mL) were prepared under inert conditions (argon). 0.9 mL aliquots were transferred to 14 suitable reaction vessels from Biotage, which were capped and placed in the autosampler of the microwave synthesizer. Polymerization was carried out at 140 °C in the microwave synthesizer (Biotage Initiator+, absorption level very high, temperature control) for varying reaction times (1 s, 10 s, 20 s, 30 s, 60 s, 90 s, 120 s, 180 s, 240 s, 300 s, 360 s, 720 s, 1080 s, and 1500 s). After automated cooling with pressurized air, the vials were opened, and aliquots were taken for analysis by means of GC, ^{1}H NMR spectroscopy and SEC.

Kinetic studies of the CROP of EtOx initiated by 4M and 3M under reflux conditions

A pre-heated flask connected to a Findenser™ with a T-piece and a gas bubbler was evacuated three times, followed by heating and subsequent cooling under an argon flow. According to an $[EtOx]_0:[initiator]_0$ ratio of 20 and a concentration of EtOx of 2 mol L^{-1}, solutions containing EtOx (5 g, 50 mmol, 20 eq.), **4M** or **3M** (576 mg, 2.5 mmol, 1 eq.) and CH_3CN (20 mL) were prepared under argon. t_0 samples for GC analysis were withdrawn. The polymerization solutions were heated using a Heat-On (Radleys) set to 85 °C to react under reflux conditions and a constant gentle flow of argon. Aliquots were taken regularly (5 min, 10 min, 15 min, 30 min, 45 min, 60 min, 90 min, 120 min, 150 min, 180 min, 240 min, 300 min, and 360 min) for analysis by means of GC, ^{1}H NMR spectroscopy and SEC.

Kinetic study of the CROP of NonOx initiated by 3M

A pre-heated flask connected to a Findenser™ with a T-piece and a gas bubbler was evacuated three times, followed by heating and subsequent cooling under an argon flow. According to a [NonOx] : [**3M**] ratio of 10 and a concentration of NonOx of 2 mol L^{-1}, NonOx (5 g, 25.3 mmol, 10 eq.) and **3M** (580 mg, 2.53 mmol, 1 eq.) were dissolved in CH_3CN (7 mL) under argon. Subsequent to sample withdrawal for GC, the polymerization solution was heated using a Heat-On (Radleys) set to 85 °C to react under reflux conditions and a constant gentle flow of argon. Aliquots were taken regularly (5 min, 10 min, 15 min, 30 min, 45 min, 60 min, 90 min, 120 min, 150 min, 180 min, 240 min, 300 min, 360 min, 420 min, 480 min, 540 min, and 600 min) for analysis by means of GC, ^{1}H NMR spectroscopy and SEC.

Synthesis of 3M-EtOx$_{20}$-OAc and 4M-EtOx$_{20}$-OAc

Reaction solutions containing EtOx, acetonitrile and **3M** or **4M** were prepared under argon to achieve an initial $[EtOx]_0 : [initiator]_0$ ratio of 20 and a concentration of EtOx of 2 mol L^{-1}. The CROP was performed either under reflux conditions or at 140 °C using a microwave synthesizer (Biotage Initiator+, absorption level very high, temperature control) as described above. Polymerization times were selected according to kinetic studies. The CROP reactions were terminated by adding acetic acid and NEt_3. The reaction solutions were stirred at 50 °C overnight, subsequently diluted with $CHCl_3$, and washed with aqueous $NaHCO_3$ solution (2×) and with brine (1×). The organic phases were dried over Na_2SO_4. After filtration, the solvent was removed under reduced pressure. The residue was dried *in vacuo*. Details are listed in Table 1.

Synthesis of 3M-NonOx$_{10}$-OAc

According to a [NonOx] : [**3M**] ratio of 10 and a concentration of NonOx of 2 mol L^{-1} in acetonitrile, a solution containing NonOx (5 g, 25.3 mmol, 10 eq.), **3M** (580 mg, 2.53 mmol, 1 eq.) and CH_3CN (7 mL) was prepared under inert conditions. The polymerization was carried out at 85 °C as described above. After 10 h (conversion: 90%), the CROP was terminated by the addition of AcOH (304 mg, 5.07 mmol, 2 eq.) and NEt_3 (513 mg, 5.07 mmol, 2 eq.). The reaction solution was stirred overnight at 50 °C and diluted with chloroform. Subsequent to washing twice with aq. $NaHCO_3$ solution and once with brine, the organic phase was dried over Na_2SO_4 and filtered. The solvent was removed under reduced pressure. After drying *in vacuo*, the product was obtained as a white powder (2.54 g, 51%).

Synthesis of 3M-EtOx$_{20}$-*b*-NonOx$_{10}$-OAc

3M (231 mg, 1.01 mmol, 1 eq.) and EtOx (2 g, 20.2 mmol, 20 eq.) were dissolved in CH_3CN (8 mL) under inert conditions ($[M]_{0,EtOx}$ = 2 mol L^{-1}). With the setup described above, the CROP was carried out at 85 °C for 16 h. Aliquots were taken and analyzed by SEC and ^{1}H NMR spectroscopy (conversion: 96%). NonOx (1.99 g, 10.1 mmol, 10 eq.) was added ($[M]_{0,NonOx}$ = 1 mol L^{-1}), and the polymerization was continued at 85 °C for 18 h (conversion: 99%). The reaction was terminated by the addition of AcOH (121 mg, 2.02 mmol, 2 eq.) and NEt_3 (204 mg, 2.02 mmol, 2 eq.). The mixture was stirred overnight at 50 °C, diluted with $CHCl_3$, and washed twice with aq. $NaHCO_3$ solution and once with brine. The organic phase was dried over Na_2SO_4. Subsequent to filtration, the volatiles were removed under reduced pressure, and the product was dried *in vacuo*. The product was obtained as a colorless powder (3.54 g, 89%).

Synthesis of 3M-NonOx$_{10}$-*b*-EtOx$_{20}$-OAc

3M (232 mg, 1.01 mmol, 1 eq.) and NonOx (2 g, 10.1 mmol, 10 eq.) were dissolved in CH_3CN (2.8 mL) under inert conditions ($[M]_{0,NonOx}$ = 2 mol L^{-1}). With the setup described above, the CROP was carried out at 85 °C for 11 h. Aliquots were taken and analyzed by ^{1}H NMR spectroscopy (conversion 99%) and SEC. EtOx (2 g, 20.0 mmol, 20 eq.) and CH_3CN (5.3 mL) were added ($[M]_{0,EtOx}$ = 2 mol L^{-1}), and the polymerization was continued at 85 °C for 17 h (conversion: 97%). The reaction was terminated by the addition of AcOH (122 mg 2.03 mmol, 2 eq.) and NEt_3 (205 mg, 2.03 mmol, 2 eq.). The mixture was stirred overnight at 50 °C. Afterwards, it was diluted with $CHCl_3$ and washed twice with aq. $NaHCO_3$ solution and once with brine. The organic phase was dried over Na_2SO_4. After filtration and removal of the volatiles under

Table 1 Detailed amounts used for the synthesis of **3M-EtOx$_{20}$-OAc** and **4M-EtOx$_{20}$-OAc**. Top: CROP conditions. Bottom: amounts used for end-capping and yields

Sample	**3M** or **4M** [mg|mmol|eq.]	EtOx [g|mmol|eq.]	CH_3CN [mL]	t_{CROP} [h]	Conversion [%]
3M-EtOx$_{20}$-OAc (reflux)	347|1.51|1	3|30.3|20	12	11	93
4M-EtOx$_{20}$-OAc (reflux)	573|2.50|1	5|50|20	20	5	Quant.
3M-EtOx$_{20}$-OAc (140 °C)	23|0.1|1	0.2|2.0|20	0.8	0.42	Quant.
4M-EtOx$_{20}$-OAc (140 °C)	21|0.09|1	0.18|1.81|20	0.72	0.42	86

Sample	AcOH [mg|mmol|eq.]	NEt_3 [mg|mmol|eq.]	Yield [g|%]
3M-EtOx$_{20}$-OAc (reflux)	136|2.27|1.5	306|3.03|2	3.30|quant.
4M-EtOx$_{20}$-OAc (reflux)	315|5.25|2.1	438|4.33|1.7	3.20|65
3M-EtOx$_{20}$-OAc (140 °C)	12.1|0.20|2	20.4|0.2|2	0.20|98
4M-EtOx$_{20}$-OAc (140 °C)	11.0|0.17|2	17.5|0.17|2	0.19|quant.

reduced pressure, the product was dried *in vacuo*. The product was obtained as a colorless powder (3.48 g, 87%).

General procedure for the synthesis of 3M-EtOx$_n$-N$_3$

According to an [EtOx] : [**3M**] ratio of 20 or 40 and a concentration of EtOx of 2 mol L^{-1} in acetonitrile, a solution containing EtOx, **3M** and CH_3CN was prepared under inert conditions. With the setup described above, the polymerization proceeded under reflux conditions (85 °C) for the time specified below. Subsequent to cooling to room temperature, an aliquot was taken to determine the conversion, and the CROP was terminated by the addition of sodium azide (NaN_3). After stirring overnight at 70 °C, the salts were filtered off. The mixture was diluted with $CHCl_3$ and washed twice with aq. $NaHCO_3$ solution and once with brine. The organic phase was dried over $MgSO_4$. After filtration, the solvent was removed under reduced pressure. The residue was dissolved in CH_2Cl_2 and precipitated in diethyl ether, which had been cooled to −80 °C in a freezer. The product was dried *in vacuo* and obtained as a colorless powder. Details are listed in Table 2.

General deprotection procedure

The polymer was dissolved in 0.1 M NaOH and stirred at room temperature overnight. The mixture was acidified to pH = 4 by addition of 1 M HCl and then extracted with $CHCl_3$ (3×). The organic phases were washed with water and brine and then dried over Na_2SO_4. Subsequent to filtration, the solvent was removed under reduced pressure, and the product was dried *in vacuo*. Details are listed in Table 3.

Results and discussion

Kinetic investigations of the CROP of EtOx

It was anticipated that the initiation behavior of the two bromomethylbenzoates **3M** and **4M** could differ due to the substitution pattern on the benzene ring at the *meta* and *para* positions, respectively. To gain initial insights into their capability to initiate the CROP, kinetic studies of the CROP of EtOx were performed. The polymerizations were conducted at an initial monomer concentration $[M]_0$ of 2 mol L^{-1} in acetonitrile at a monomer to initiator ($[M]_0/[I]_0$) ratio of 20 to enable straightforward characterization with a focus on the end groups. To ensure consistent reaction conditions for both initiators, the reactions were carried out first at 140 °C using a microwave synthesizer. CROP performed under these conditions is known to promote the formation of proton-initiated species through chain transfer reactions.[28–30] Considering the importance of the α-end group, kinetic studies were also conducted under reflux conditions, *i.e.*, at 85 °C. In all cases, the progress of the polymerization was monitored by means of ^{1}H NMR spectroscopy and GC to determine the initiator and monomer conversions, respectively. The molar masses and dispersities of the formed PEtOx were assessed by SEC.

The first-order kinetic plot with respect to monomer concentration revealed a linear progression for the CROP initiated with both initiators when conducted at 140 °C, pointing towards pseudo-first-order kinetics with the propagation as the rate-determining step (Fig. 2). The polymerization rate constants determined from the slope of the linear regression were fairly similar (k_p, **4M** = 2.05 L mol^{-1} min^{-1}; k_p, **3M** = 1.93 L mol^{-1} min^{-1}) because the monomer, bromide counterion, solvent and temperature were the same. Both rate constants are similar to the value of the CROP of EtOx initiated by methyl bromoacetate conducted under the same conditions ($k_p \approx 2.7$ L mol^{-1} min^{-1}).[25] Likewise, the polymerization rate constants were similar when the CROP was performed at 85 °C (k_p, **4M** = 0.053 L mol^{-1} min^{-1}; k_p, **3M** = 0.047 L mol^{-1} min^{-1}).

Signals in the SEC elugrams shifted towards higher molar masses with increasing polymerization time. A linear increase of the molar mass with conversion was observed for both initiators throughout the polymerization regardless of the

Table 2 Detailed amounts used for the synthesis of **3M-EtOx$_n$-N$_3$**. Top: CROP conditions. Bottom: amounts used for end-capping and yields

Sample	**3M** [mg|mmol|eq.]	EtOx [g|mmol|eq.]	CH_3CN [mL]	t_{CROP} [h]	Conversion [%]
3M-EtOx$_{20}$-N$_3$	578|2.52|1	5|50.4|20	20	17.5	92
3M-EtOx$_{40}$-N$_3$	290|1.26|1	5|50.4|40	20	37.5	98

Sample	NaN_3 [mg|mmol|eq.]	Yield [g|%]
3M-EtOx$_{20}$-N$_3$	434|6.56|2.6	3.44|69
3M-EtOx$_{40}$-N$_3$	219|3.28|2.6	4|80

Table 3 Detailed amounts for the hydrolysis of the methyl ester α-end group

Sample	Educt	Amount educt [g|mmol]	0.1 M NaOH [mL]	Yield [g|%]
3A-EtOx$_{20}$-OH	**3M-EtOx$_{20}$-OAc** (reflux)	0.50|0.26	5.1	0.32|64
4A-EtOx$_{20}$-OH	**4M-EtOx$_{20}$-OAc** (reflux)	0.51|0.27	5.6	0.11|22
3A-EtOx$_{20}$-N$_3$	**3M-EtOx$_{20}$-N$_3$**	3.06|1.55	30	3.02|99
3A-EtOx$_{40}$-N$_3$	**3M-EtOx$_{40}$-N$_3$**	3.60|0.91	36	3.56|99

CROP conditions. As commonly observed, molar mass distributions were narrower when the CROP was performed at 85 °C ($Đ_{140°C} \leq 1.26$; $Đ_{85°C} \leq 1.21$). For both polymerization temperatures, dispersities were slightly lower when the *meta*-substituted **3M** was used ($Đ_{140°C} \leq 1.20$; $Đ_{85°C} \leq 1.13$).

This observation might be reasoned by slight differences in the initiation rate of the CROP when initiated with **3M** or **4M**. We hence thoroughly inspected data describing the early stages of the CROP. Indeed, data points at $t \leq 10$ min in the pseudo-first-order kinetic plot of the CROP initiated by **4M** at 85 °C hinted at a slow initiation. In addition, changes in the aromatic region of the ^{1}H NMR spectra throughout the course of the polymerization were detected for all CROP (Fig. S4–S7). In particular, the proton signals at C3 and C5 of the aromatic ring of **4M** (δ = 7.46 ppm) were shifted upfield upon initiation. Also, the benzylic methylene proton signal at δ = 4.51 ppm shifted for both initiators. The corresponding signals of unreacted **3M** as well as **4M** remained fairly separated from signals assigned to the end groups of the formed PEtOx and residual monomer. As the chemical shift of the methyl ester proton signal at δ = 3.91 ppm remained unaltered, integrals of these peaks were used to estimate initiator efficiencies throughout the course of all CROP (Fig. 2, bottom).

For the CROP performed at 140 °C, initiator efficiencies above 90% were observed early in the reaction. Fluctuations in later stages of the CROP are most likely due to the inaccuracy of the integration. The initiation was slower for the CROP performed at 85 °C. **3M** was converted faster than **4M**, as is particularly evident in a first-order kinetic plot regarding initiator concentration (Fig. S8).

Benzyl bromides are substrates for nucleophilic substitutions that can favor both S_N1 and S_N2 reaction mechanisms. On the one hand, their resonance stabilization favors the formation of a benzyl cation *via* an S_N1 reaction. On the other hand, the primary carbon atom in benzyl substrates can promote an S_N2 reaction. The fact that acetonitrile represents a non-protic solvent is likely to push the mechanism towards S_N2 or a mixed type in the present case. As depicted in Fig. S8, the consumption of the initiator does not follow a first-order law. Hence, the initiation step is not purely an S_N1-type nucleophilic substitution.

The lower reactivity of **4M** is in agreement with its unfavorable resonance structure in that a positive charge is in direct neighborhood with the partial positive charge at the benzylic position (Scheme S1). The slower initiation of **4M** also explains the slightly elevated dispersity values of the formed PEtOx, as macromolecules formed by delayed initiation feature lower molar masses.

Determination of the α-end group fidelity

The presence or absence of the functional moiety of interest is of significant importance when designing end-functionalized polymers. The α-end group fidelity of POx can be affected by chain transfer reactions taking place during the CROP (Scheme S2). In such reactions, a proton is abstracted from C1 of the substituent at the ω-terminal oxazolinium ion. A C–C double bond is formed through this elimination. The released proton can initiate a new chain, resulting in POx featuring a hydrogen atom as the α-end group. To determine the α-end group fidelity, the CROP was terminated with acetic acid and triethylamine to introduce an acetate ω-end group. The resulting **3M-EtOx$_{20}$-OAc** and **4M-EtOx$_{20}$-OAc** were characterized in detail by ^{1}H NMR spectroscopy, SEC, MALDI-TOF MS and HPLC to investigate the presence of the desired methyl ester in the PEtOx initiated by **3M** and **4M**, respectively (Table 4).

Signals assigned to both new α-end groups were detected in the ^{1}H NMR spectra of all PEtOx, regardless of the polymerization temperature and the initiator, *i.e.*, **3M** or **4M**. In addition, the peak integrals were in line with those of the acetate ω-end groups (Fig. S9 and 10). However, the end group fidelity cannot be assessed *via* this approach as chains with the desired α-end group may also feature an ω-end group other than acetate. Conversely, chains with an acetate ω-end group may also be proton initiated. MALDI-TOF mass spectrometry confirmed the covalent attachment of the methyl ester moiety in all PEtOx (Fig. S11 and S12). In fact, the most abundant species corresponded to the envisaged product. In particular, mass spectra of PEtOx produced at 140 °C revealed the presence of proton-initiated species as a result of chain transfer reactions. This observation is consistent with prior knowledge and is also indicated by a slight low molar mass tailing visible in the SEC elugrams of **3M-EtOx$_{20}$-OAc** and **4M-EtOx$_{20}$-OAc** synthesized at 140 °C (Fig. S13). Unfortunately, the amount of the proton-initiated chains cannot be quantified from the mass spectra as preferential ionization of chains with certain end groups might occur.

Although rarely applied to elucidate the end group fidelity in the research field, HPLC is well capable of distinguishing between proton-initiated and initiator-derived PEtOx chains for benzylic initiators as well as methyl tosylate.[28] The previously established HPLC methods using an RP18 Chromolith column were only slightly adjusted here.[28,31] Measurements were conducted using a binary mobile-phase gradient comprising a mixture of water and acetonitrile, with the addition of 0.1% formic acid to improve signal resolution. The elugrams depicted in Fig. 3 were recorded utilizing an ELSD.

The elugrams of **3M-EtOx$_{20}$-OAc** and **4M-EtOx$_{20}$-OAc** synthesized under reflux conditions each revealed only one main signal. In contrast, two polymer populations were visible in the elugrams of the respective polymers synthesized at 140 °C. To identify the structure of the underlying species, fractions were collected from the eluate and analyzed by means of MALDI-TOF MS. The signals eluting at 9.3 min corresponded to the proton-initiated species, whereas the main products bearing the α-methyl ester moieties eluted at 10.9 min, irrespective of the substitution pattern on the α-terminal benzene ring. This order of elution is in accordance with the hydrophobicity of the α-end groups as the more hydrophobic aromatic methyl esters are expected to interact more strongly with the hydrophobic column material than chains lacking this moiety. The fact that **4M-EtOx$_{20}$-OAc** contained a larger amount of proton-initiated chains than **3M-EtOx$_{20}$-OAc** is in agreement with the strong molar mass tailing observed in the SEC

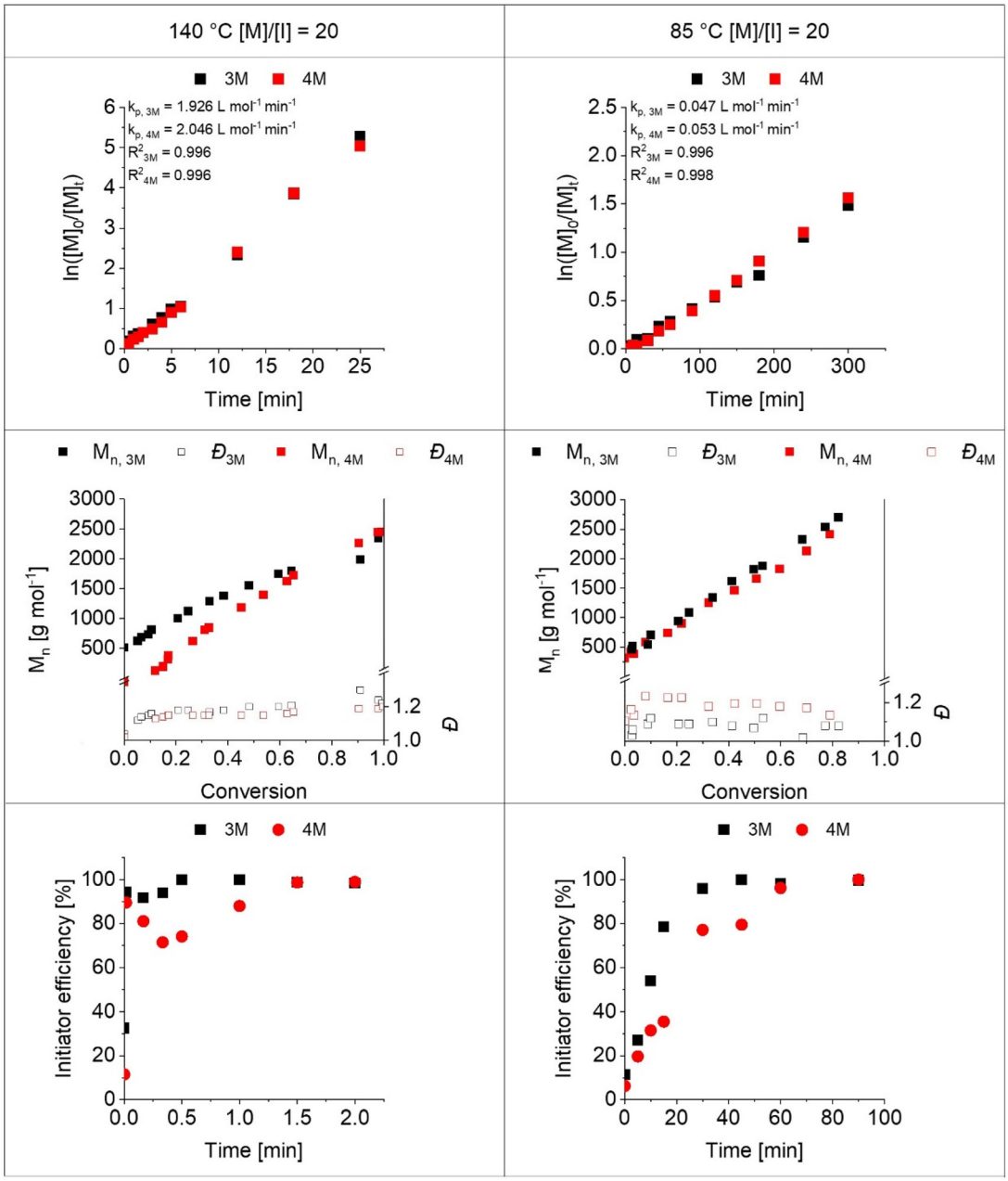

Fig. 2 Kinetic studies of the CROP of EtOx initiated by **3M** (black) and **4M** (red) at 140 °C as well as at 85 °C ($[M]_0/[I]_0$ = 20, $[M]_0$ = 2 mol L^{-1} in CH_3CN). Top: first-order kinetic plot according to $\ln([M]_0/[M]_t) = k_p \times [I]_0 \times t$. Monomer concentrations were determined by GC. Middle: evolution of the molar masses M_n and dispersities $Đ$ (SEC, RID, PS calibration) with monomer conversion. Bottom: initiator efficiencies estimated by ^{1}H NMR spectroscopy.

elugram of the sample. According to signal areas, the samples synthesized at 140 °C contained more than 20% of the undesired impurity, consistent with previously reported studies on the synthesis of POx at 140 °C.[28,29] Irrespective of the initiator, the signals assigned to proton-initiated chains were below the detection limit of the HPLC method (Fig. S14) when the CROP was conducted at 85 °C.

As the initiation of the CROP using **3M** was slightly faster than that of **4M**, all further experiments were performed using **3M** as the initiator at 85 °C.

Synthesis of amphiphilic block copolymers

To establish a framework for the synthesis of amphiphilic block copolymers, the initiator **3M** was tested with a hydrophobic monomer, *i.e.*, 2-*n*-nonyl-2-oxazoline (NonOx). Initially, the CROP was attempted in chlorobenzene at 135 °C (Fig. S15). As broad molar mass distributions caused by delayed initiation were observed, the solvent was switched to acetonitrile under reflux conditions (Fig. S16 and S17).[7,32] To ensure the solubility of the formed PNonOx in acetonitrile, $[M]_0/[I]_0$ = 10 was

Table 4 Selected characterization data of POx obtained by initiation of the CROP with **3M** or **4M**, respectively

Sample	$M_{n,theo}$ [a] [g mol^{-1}]	$M_{n,SEC}$ [b] [g mol^{-1}]	$Đ_{SEC}$ [b]	$M_{n,MALDI}$ [c] [g mol^{-1}]	$Đ_{MALDI}$ [c]	Purity[d] [%]
3M-EtOx$_{20}$-OAc (reflux)	1890	2700	1.10	2200	1.08	99
4M-EtOx$_{20}$-OAc (reflux)	1890	2100	1.08	2260	1.07	95
3M-EtOx$_{20}$-OAc (140 °C)	2090	2600	1.09	1870	1.12	79
4M-EtOx$_{20}$-OAc (140 °C)	2090	2100	1.23	2220	1.07	65
3M-NonOx$_{10}$-OAc	1790	2800	1.10	1880	1.24	n.d.
3M-EtOx$_{20}$-*b*-NonOx$_{10}$-OAc	4060	5100	1.10	4000	1.13	n.d.
3M-NonOx$_{10}$-*b*-EtOx$_{20}$-OAc	4060	4900	1.15	4010	1.12	n.d.
3M-EtOx$_{20}$-N$_3$	1980	2700	1.14	2430	1.22	95
3M-EtOx$_{40}$-N$_3$	3960	4200	1.11	4190	1.10	93
3A-EtOx$_{20}$-OH	1880	1500	1.13	2300	1.07	100
4A-EtOx$_{20}$-OH	1880	1400	1.13	2010	1.07	100
3A-EtOx$_{20}$-N$_3$	1970	1300	1.08	2620	1.07	93
3A-EtOx$_{40}$-N$_3$	3950	3800	1.10	4040	1.10	87

[a] Determined according to $M_{n,theo} = [M]_0/[I]_0 \times$ conversion. [b] Determined by SEC (RID, PS calibration). [c] Determined from the MALDI-TOF mass spectra (DCTB + NaTFA). [d] Determined from the signal areas of HPLC chromatograms (c = 1 mg mL^{-1}).

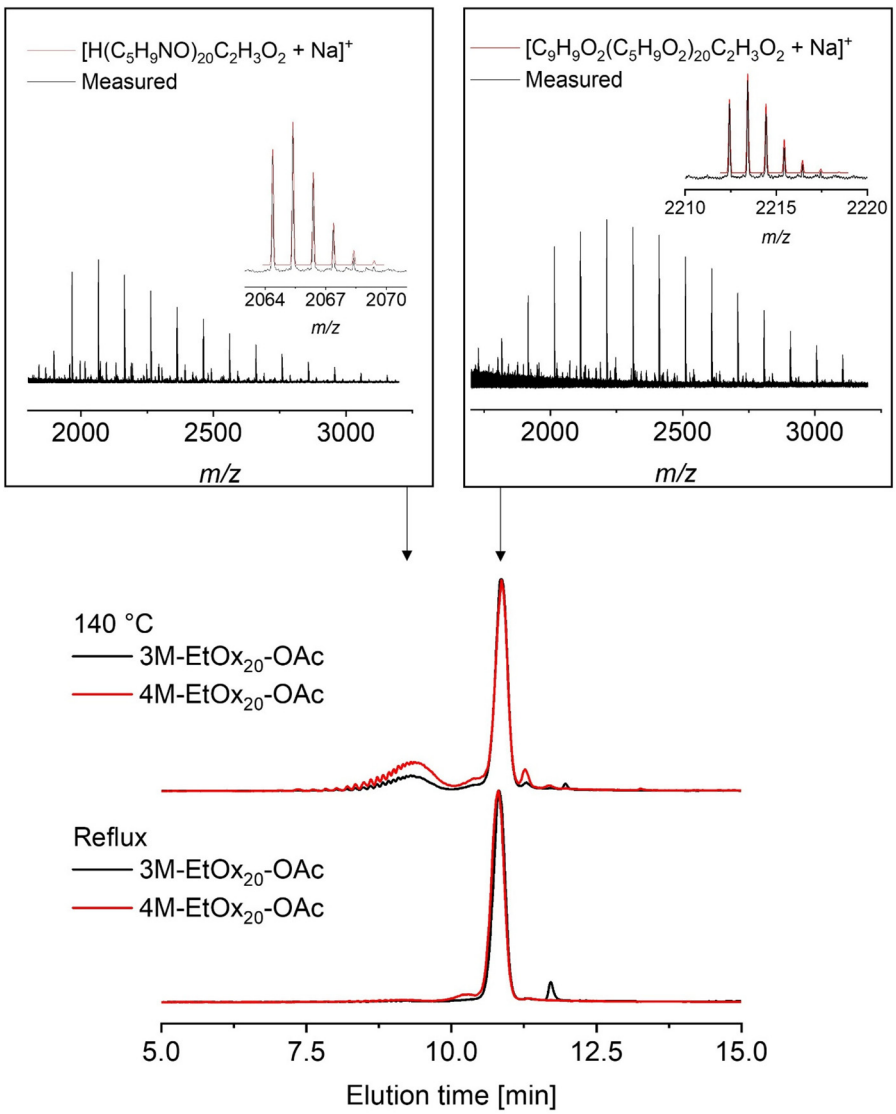

Fig. 3 α-End group determination using HPLC and MALDI-TOF MS for PEtOx initiated by **3M** (black) and **4M** (red) under microwave (140 °C) and reflux (85 °C) conditions. Bottom: HPLC chromatograms of **3M-EtOx$_{20}$-OAc** and **4M-EtOx$_{20}$-OAc** (RP18 Chromolith column, water/acetonitrile gradient with 0.1% formic acid, ELSD). Top: full MALDI mass spectra of HPLC fractions collected during the measurement of **4M-EtOx$_{20}$-OAc**. The insets show overlays of measured and theoretical isotopic patterns for signal assignments.

chosen. The initiation proceeded faster than in chlorobenzene, but slower than that of EtOx, as evident from the first-order kinetic plot as well as from initiator efficiencies. After 45 min, the latter reached around 90%. Data points from there on were taken to estimate the k_p value of 0.039 L mol^{-1} min^{-1}. Despite the delayed initiation, dispersities remained below 1.2. Also, the termination of the CROP with triethylammonium acetate proceeded smoothly, as verified by ^{1}H NMR spectroscopy and MALDI-TOF MS (Fig. S18–S20). Proton-initiated species were not detected in the mass spectrum, but the ω-end group was prone to fragmentation, as often observed for PNonOx with ester ω-end groups.[33,34]

As a result, block copolymers composed of EtOx and NonOx were synthesized in CH_3CN at 85 °C, *i.e.*, reflux conditions. Sticking to the $[M]_0/[I]_0$ ratios utilized in the kinetic studies, EtOx and NonOx were polymerized by consecutive monomer addition. Depending on the targeted application, the presence of the methyl ester at the α-chain end could be favorable for functionalization at either the hydrophilic or the hydrophobic block copolymer segment. Consequently, either EtOx or NonOx was polymerized as the first monomer. Again, the CROP was terminated using *in situ*-formed triethylammonium acetate. ^{1}H NMR spectroscopy confirmed the presence of both repeating units in the intended molar ratios in both block copolymers (Fig. S21, $F_{NonOx,theo.}$ = 0.33, $F_{NonOx,NMR}$ = 0.35 to 0.37), and end-group signals were detected as well.

The chain extensions were evidenced by a shift of the SEC signals towards lower elution volumes after polymerization of the second block (Fig. 4). For both block copolymers, SEC elugrams demonstrated narrow molar mass distributions with dispersity values of $Đ$ = 1.10 and 1.15 for **3M-EtOx$_{20}$-*b*-NonOx$_{10}$-OAc** and **3M-NonOx$_{10}$-*b*-EtOx$_{20}$-OAc**, respectively. The slightly elevated dispersity of **3M-NonOx$_{10}$-*b*-EtOx$_{20}$-OAc** is due to a small shoulder at higher elution volume. One might

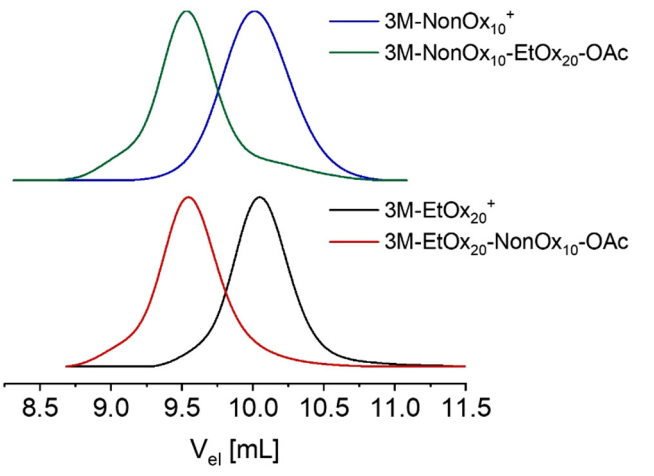

Fig. 4 SEC elugrams (RI detection) of **3M-NonOx$_{10}$-*b*-EtOx$_{20}$-OAc** and **3M-EtOx$_{20}$-*b*-NonOx$_{10}$-OAc** as well as of the corresponding first blocks **3M-NonOx$_{10}^+$** and **3M-EtOx$_{20}^+$** before the addition of the second monomer.

assume that the re-initiation from the **NonOx$_{10}$** species was incomplete, which would be in accordance with the higher k_p value of EtOx used for chain extension. However, MALDI-TOF mass spectrometry revealed a distribution assigned to $[H(C_5H_9NO)_{10}C_2H_3O_2 + Na]^+$ at low *m*/*z* values (Fig. S22), *i.e.*, PEtOx chains formed through chain transfer. In contrast, no proton-initiated PNonOx was detected in the MALDI-TOF mass spectrum of **3M-EtOx$_{20}$-*b*-NonOx$_{10}$-OAc**. In addition, both mass spectra revealed the presence of homopolymers of the second block, which were most likely formed through fragmentation due to the higher laser intensities required during the measurements.

At higher *m*/*z* values, unfragmented block copolymers containing the desired end groups (**3M** and -OAc) were identified in both samples. In analogy to the homopolymers, the mass spectrum of **3M-EtOx$_{20}$-*b*-NonOx$_{10}$-OAc** revealed a higher abundance of oxazolinium species than the block copolymer in which EtOx is the terminal block. An additional unknown block copolymer species was also detected, which might originate from fragmentation due to the high laser intensities that were required to ionize the samples.

Synthesis of heterotelechelic polymers and deprotection

An additional functional group of orthogonal reactivity could broaden the use of POx with a methyl ester α-end group and enable further modification in the context of biomedical applications. To obtain such heterotelechelic POx, the CROP was initiated with **3M** at $[M]_0/[I]_0$ ratios of 20 and 40 under reflux conditions and subsequently terminated with sodium azide to implement an azide ω-end group. Again, ^{1}H NMR spectroscopy confirmed the α-end group but was not suitable for detecting the azide ω-end group. IR spectroscopy was employed for this purpose, revealing the characteristic azide vibrational band at around 2100 cm^{-1} (Fig. 5). In addition, *m*/*z* series assigned to species with an azide end group or its fragments were found in the MALDI-TOF mass spectra (Fig. S27 and S28).

The methyl ester α-end groups may be valuable for transesterification or amidation reactions for further modifications of interest. For other reactions, such as carbodiimide-mediated coupling of peptides, free carboxylic acid groups are more favored.[35–38] Consequently, the heterotelechelic **3M-EtOx$_{20}$-N$_3$**, **3M-EtOx$_{40}$-N$_3$**, **3M-EtOx$_{20}$-OAc** and **4M-EtOx$_{20}$-OAc** were deprotected by hydrolysis with 0.1 M aqueous NaOH solution at room temperature overnight.

^{1}H NMR spectroscopy indicated the disappearance of the methyl ester signal around δ = 4.00 ppm for all deprotected PEtOx, whereas the amide moieties in the PEtOx backbone remained unaffected (Fig. 5). Also, the ester-based ω-end group of **3M-EtOx$_{20}$-OAc** and **4M-EtOx$_{20}$-OAc** was hydrolyzed during deprotection as the methyl signals of the acetate were absent in the ^{1}H NMR spectra (Fig. S29 and S30). The adjacent methylene proton signal shifted, indicating the formation of a hydroxyl ω-end group. In contrast, the azide ω-end groups remained stable as seen in the IR spectra of **3A-EtOx$_{20}$-N$_3$** and **3A-EtOx$_{40}$-N$_3$**. In accordance with the hydrolysis of the methyl ester to yield a carboxylic acid, a slight shift of the respective

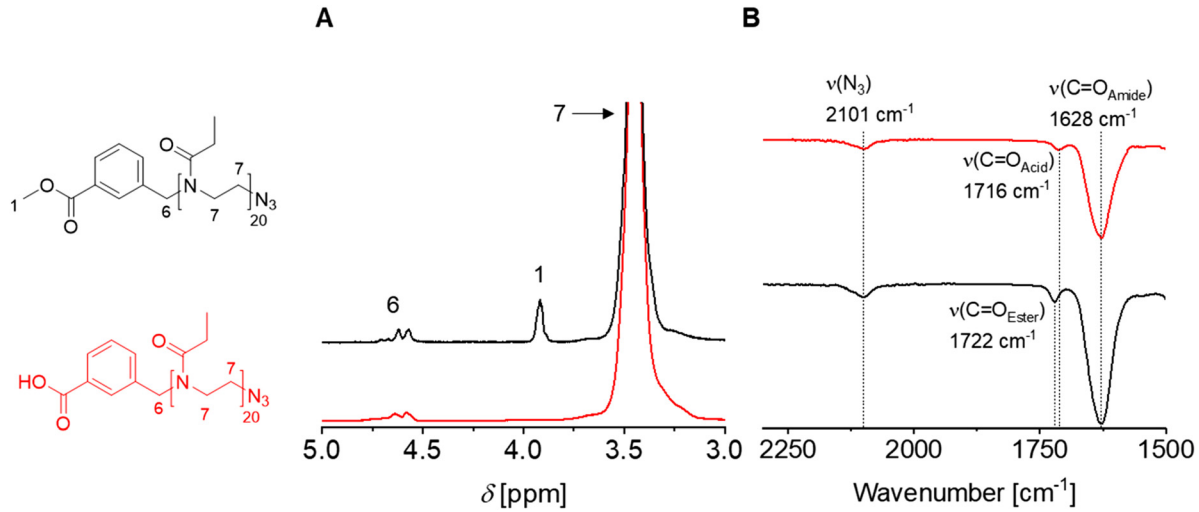

Fig. 5 Spectroscopic confirmation of end groups in the heterotelechelic **3M-EtOx$_{20}$-N$_3$** (black) and **3A-EtOx$_{20}$-N$_3$** (red). (A) Overlay of ^{1}H NMR spectra ($CDCl_3$, 300 MHz). (B) Overlay of IR spectra with assignment of characteristic vibrational bands. Full spectra are shown in the SI.

C═O vibrational band was observed in the IR spectra of all deprotected polymers. However, the amide bands remained unchanged, showing the preservation of the PEtOx backbone.

The observations discussed above are in agreement with the results from MALDI-TOF mass spectrometry, which clearly indicated the presence of hydroxyl ω-end groups in **3A-EtOx$_{20}$-OH** and **4A-EtOx$_{20}$-OH**. In addition to species with carboxylic acid α-end groups, sodium carboxylates were ionized in all deprotected PEtOx (Fig. S31–S34).

Surprisingly, the end group transformation upon deprotection significantly affected the elution behavior during SEC analysis (Fig. 6 and Fig. S35). While the molar mass distributions remained narrow and unimodal ($Đ \leq 1.13$), the increased end-group polarity led to a decrease in hydrodynamic volume in the chloroform-based eluent. The apparent molar masses determined by polystyrene calibration thus decreased to a larger extent than expected, in particular for PEtOx with a DP value of 20 (Table 4).

The influence of the end group conversion on the elution behavior was even more pronounced during HPLC analysis on a C18 column. All deprotected polymers eluted earlier than their protected counterparts. This is reasonable because the more polar carboxylic acid end groups would interact less with the hydrophobic stationary phase than the corresponding methyl esters. The influence was diminished upon an increase of the DP value, as seen from a comparison of the elution time differences between protected and deprotected polymers with azide ω-end groups. The difference in retention behavior was particularly prominent for **3M-EtOx$_{20}$-OAc** and **3A-EtOx$_{20}$-OH** due to the additional contribution of the altered ω-end groups. Here, the combination of two hydrophilic end groups and a comparatively low molar mass even led to slight differences in elution times of oligomer chains with distinct DP values.

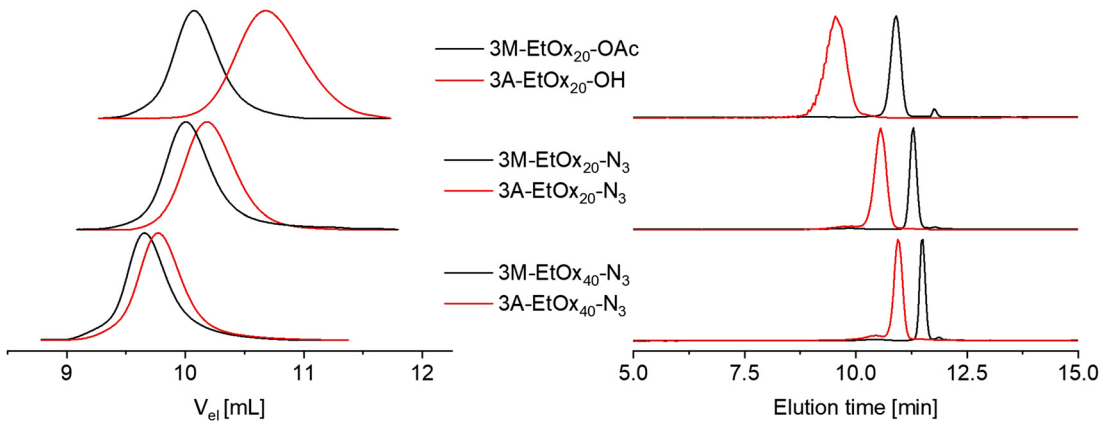

Fig. 6 Chromatographic analysis of protected and deprotected PEtOx heterotelechelics obtained by initiation of CROP with **3M**. Left: SEC (RID). Right: HPLC (RP18 Chromolith column, water/acetonitrile gradient with 0.1% formic acid, ELSD).

Conclusion

Two commercially available bromomethylbenzoates, **3M** and **4M**, were used as initiators for the CROP of 2-oxazolines, thereby introducing a methyl ester α-end group. Kinetic studies revealed similar propagation rates for the CROP initiated by the two compounds at 140 °C as well as at 85 °C. However, **3M** exhibited slightly faster initiation when the CROP was conducted under reflux conditions. In-depth HPLC analysis of the synthesized polymers revealed pronounced formation of proton-initiated chains when the CROP was carried out at 140 °C, but the chain transfer was almost absent when the CROP was performed under reflux conditions in acetonitrile. Subsequent syntheses of heterotelechelic polymers and block copolymers showed that the synthesis of more complex structures was also possible using this initiator system. Furthermore, deprotection of the methyl ester group to yield the free carboxylic acid was successfully achieved while preserving azide ω-end groups.

In summary, the commercial initiator enabled a straightforward introduction of a methyl ester or carboxylic acid functionality at the α-chain end of various POx, facilitating further modification of the polymers with, *e.g.*, small molecules or other polymeric building blocks. In particular, the heterotelechelic polymers appear highly promising for this purpose due to the orthogonal reactivity of carboxylic acid or methyl ester and azide end groups. The novel and versatile end-functionalized POx will be vital for biomedical applications as the significance of POx as a PEG replacement has triggered a need for end-functionalized building blocks.

Author contributions

Caroline T. Holick: formal analysis, investigation, visualization, and writing – original draft; Nora Engel: conceptualization, formal analysis, investigation, and writing – review & editing; Nicole Fritz: investigation and writing – review & editing; Christine Weber: conceptualization, supervision, and writing – original draft; Ulrich S. Schubert: funding acquisition, supervision, and writing – review & editing.

Conflicts of interest

The authors declare that they have no known competing financial interests that could have appeared to influence this work.

Data availability

The data that support the findings of this study are available in the supplementary information (SI) of this article. Supplementary information is available: ^{1}H NMR spectra of all compounds, ^{1}H NMR spectra recorded during the kinetic studies, IR spectra of azide-functionalized polymers, SEC elugrams of all polymers, SEC elugrams taken during kinetic studies, additional kinetic plots, MALDI mass spectra of all polymers, additional HPLC elugrams and ELSD linearity test, Schemes depicting resonance structures of the initiators and the chains transfer mechanism. See DOI: https://doi.org/10.1039/d6py00309e.

Acknowledgements

This work was funded by the German Federal Ministry for Economic Affairs and Energy (BMWE, project BASE-Lipid, grant number 16LP401003) and Thüringer Aufbaubank (TAB, "Innovative Pharmapolymers", grant number 2021FGI0005). The MALDI-TOF mass spectrometer (rapifleX) was funded by the TAB (grant number 2016IZN0009). We acknowledge NGP Polymers GmbH for providing the monomer NonOx.

References

1 C. Bento, M. Katz, M. M. M. Santos and C. A. M. Afonso, *Org. Process Res. Dev.*, 2024, **28**, 860–890.
2 M. F. S. Deuker, V. Mailänder, S. Morsbach and K. Landfester, *Nanoscale Horiz.*, 2023, **8**, 1377–1385.
3 D. Pizzi, J. Humphries, J. P. Morrow, A. M. Mahmoud, N. L. Fletcher, S. E. Sonderegger, C. A. Bell, K. J. Thurecht and K. Kempe, *Biomacromolecules*, 2023, **24**, 246–257.
4 S. Jana and R. Hoogenboom, *Polym. Int.*, 2022, **71**, 935–949.
5 A.-S. Glaive, C. L. Cœur, J.-M. Guigner, C. Amiel and G. Volet, *Langmuir*, 2024, **40**, 2050–2063.
6 K. Lava, B. Verbraeken and R. Hoogenboom, *Eur. Polym. J.*, 2015, **65**, 98–111.
7 B. Verbraeken, B. D. Monnery, K. Lava and R. Hoogenboom, *Eur. Polym. J.*, 2017, **88**, 451–469.
8 G. Delaittre, *Eur. Polym. J.*, 2019, **121**, 109281.
9 Z. A. I. Mazrad, M. Lai, T. P. Davis, J. A. Nicolazzo, K. J. Thurecht, M. N. Leiske and K. Kempe, *Polym. Chem.*, 2022, **13**, 4436–4445.
10 S. Osawa, T. Ishii, H. Takemoto, K. Osada and K. Kataoka, *Eur. Polym. J.*, 2017, **88**, 553–561.
11 J. Kim, V. Beyer and C. R. Becer, *Macromolecules*, 2022, **55**, 10651–10661.
12 L. Daoud, S. Hoang, A. Milin-Moguerou, J. Eyer, T. Breton, V. Montembault, L. Fontaine, C. Passirani, P. Saulnier and O. Krupka, *Biomacromolecules*, 2025, **26**, 1923–1934.
13 S. Jana, M. Roels, M. N. Leiske, Y. Bernhard, B. G. De Geest, K. Van Hecke and R. Hoogenboom, *Angew. Chem., Int. Ed.*, 2025, **64**, e202424873.
14 O. Krupka, V. Montembault, L. Fontaine and P. Hudhomme, *Eur. Polym. J.*, 2026, **247**, 114584.
15 G. Gil Alvaradejo, M. Glassner, R. Kumar, V. Trouillet, A. Welle, Y. Wang, V. R. de la Rosa, S. Sekula-Neuner, M. Hirtz, R. Hoogenboom and G. Delaittre, *Macromol. Rapid Commun.*, 2020, **41**, 2000320.
16 K. Kempe, S. Onbulak, U. S. Schubert, A. Sanyal and R. Hoogenboom, *Polym. Chem.*, 2013, **4**, 3236–3244.

17 A.-L. Ziegler, A. Kerr, F. T. Kaps and R. Luxenhofer, *Polym. Chem.*, 2025, **16**, 1383–1392.
18 M. Glassner, S. Maji, V. R. de la Rosa, N. Vanparijs, K. Ryskulova, B. G. De Geest and R. Hoogenboom, *Polym. Chem.*, 2015, **6**, 8354–8359.
19 A. Tantipanjaporn and M.-K. Wong, *Molecules*, 2023, **28**, 1083.
20 P. J. M. Bouten, D. Hertsen, M. Vergaelen, B. D. Monnery, M. A. Boerman, H. Goossens, S. Catak, J. C. M. van Hest, V. Van Speybroeck and R. Hoogenboom, *Polym. Chem.*, 2015, **6**, 514–518.
21 A. Levy and M. Litt, *J. Polym. Sci. Part A-1 Polym. Chem.*, 1968, **6**, 1883–1894.
22 C. T. Holick, T. Klein, C. Mehnert, F. Adermann, I. Anufriev, M. Streiber, L. Harder, A. Traeger, S. Hoeppener, C. Franke, I. Nischang, S. Schubert and U. S. Schubert, *Small*, 2025, **21**, 2411354.
23 S. Zalipsky, C. B. Hansen, J. M. Oaks and T. M. Allen, *J. Pharm. Sci.*, 1996, **85**, 133–137.
24 M. C. Woodle, C. M. Engbers and S. Zalipsky, *Bioconjugate Chem.*, 1994, **5**, 493–496.
25 A. Podevyn, K. Arys, V. R. de la Rosa, M. Glassner and R. Hoogenboom, *Eur. Polym. J.*, 2019, **120**, 109273.
26 R. M. England, J. I. Hare, P. D. Kemmitt, K. E. Treacher, M. J. Waring, S. T. Barry, C. Alexander and M. Ashford, *Polym. Chem.*, 2016, **7**, 4609–4617.
27 T. Saegusa, S. Kobayashi and A. Yamada, *Makromol. Chem.*, 1976, **177**, 2271–2283.
28 M. Brunzel, M. Dirauf, M. Sahn, J. A. Czaplewska, N. Fritz, C. Weber, I. Nischang and U. S. Schubert, *J. Chromatogr. A*, 2021, **1653**, 462364.
29 F. J. Arraez, X. Xu, P. H. M. Van Steenberge, V.-V. Jerca, R. Hoogenboom and D. R. D'hooge, *Macromolecules*, 2019, **52**, 4067–4078.
30 M. Sahn, D. Bandelli, M. Dirauf, C. Weber and U. S. Schubert, *Macromol. Rapid Commun.*, 2017, **38**, 1700396.
31 N. Engel, M. Dirauf, J. A. Czaplewska, I. Nischang, M. Gottschaldt and U. S. Schubert, *R. Soc. Open Sci.*, 2024, **11**, 231008.
32 R. Hoogenboom, M. W. M. Fijten and U. S. Schubert, *J. Polym. Sci., Part A: Polym. Chem.*, 2004, **42**, 1830–1840.
33 C. Weber, M. Wagner, D. Baykal, S. Hoeppener, R. M. Paulus, G. Festag, E. Altuntas, F. H. Schacher and U. S. Schubert, *Macromolecules*, 2013, **46**, 5107–5116.
34 J. Meyer, N. E. Göppert, L. M. Stafast, C. Weber and U. S. Schubert, *Macromol. Rapid Commun.*, 2025, **46**, e00273.
35 N. A. Hutter, M. Steenackers, A. Reitinger, O. A. Williams, J. A. Garrido and R. Jordan, *Soft Matter*, 2011, **7**, 4861–4867.
36 A. Mero, G. Pasut, L. D. Via, M. W. M. Fijten, U. S. Schubert, R. Hoogenboom and F. M. Veronese, *J. Controlled Release*, 2008, **125**, 87–95.
37 O. Sedlacek, V. R. de la Rosa and R. Hoogenboom, *Eur. Polym. J.*, 2019, **120**, 109246.
38 M. Miyamoto, K. Naka, M. Shiozaki, Y. Chujo and T. Saegusa, *Macromolecules*, 1990, **23**, 3201–3205.